SUPPORTING INFORMATION

All inorganic made coordination polymers have been possible with the *m*-carboranylphosphinate ligand.

Elena Oleshkevich,[a] Isabel Romero,[b] Francesc Teixidor[a] and Clara Viñas,[a,*].

[a] Institut de Ciència de Materials de Barcelona (ICMAB-CSIC), Campus UAB, 08193 Bellaterra, Spain.

[b] Departament de Química, Universitat de Girona, Campus de Montilivi, E-17003 Girona, Spain.

Figure S1. IR spectra of compounds a) **4**, b) **6**, c) **7**, d) **8**, e) **9**, and comparison of IR spectra of compounds f) **1** and **2**, g) **3** and **9**, h) **2** and **9**.

Figure S2. ^{11}B-NMR and ^{11}B{^{1}H}-NMR spectra of the compound **4.**

Figure S3. ^{11}B-NMR and ^{11}B{^{1}H}-NMR spectra of the compound **6**.

Figure S4. ^{1}H-NMR, ^{1}H{^{11}B}-NMR, ^{11}B-NMR, ^{11}B{^{1}H}-NMR, ^{31}P-NMR, ^{13}C{^{1}H}-NMR spectra of the compound **7**.

Figure S5. ^{1}H-NMR, ^{1}H{^{11}B}-NMR, ^{11}B-NMR, ^{11}B{^{1}H}-NMR, ^{31}P-NMR, ^{13}C{^{1}H}-NMR spectra of the compound **8**.

Figure S6. ^{11}B-NMR and ^{11}B{^{1}H}-NMR spectra of the compound **9**.

Figure S7. Evolution of the ^{11}B{^{1}H}-NMR spectrum of compound **3** in MeOH/H_2O to produce lower nuclearity species.

Figure S8. Packing structure of Cd polymer **8.**

Figure S9. X-ray powder diffraction (XRPD) of **6** (a) (Cu complex) and **7** (b) (Zn complex).

Figure S10. Thermal gravimetric analysis (TGA/DCS) of a) **6**; b) **7**; c) **8**.

Figure S14. EPR of a) **1**, b) **2** and c) **3** at different temperatures on powder samples.

Table S1. Crystal Data for X-ray structures of Co complex **4**.

Table S2. Selected bond lengths (Å) and angles (°) for Co complex **4**.

Table S3. Crystal Data for X-ray structures of Cd complex **8**.

Table S4. Selected bond lengths (Å) and angles (°) for Cd complex **8**.

Table S5. Thermal gravimetric analysis (TGA) data for compounds **1**-**3**, **6**-**8**.

Figure S1. IR spectra of compounds a) **4**, b) **6**, c) **7**, d) **8**, e) **9**, and comparison of IR spectra of compounds f) **1** and **2**, g) **3** and **9**, h) **2** and **9.**

a)

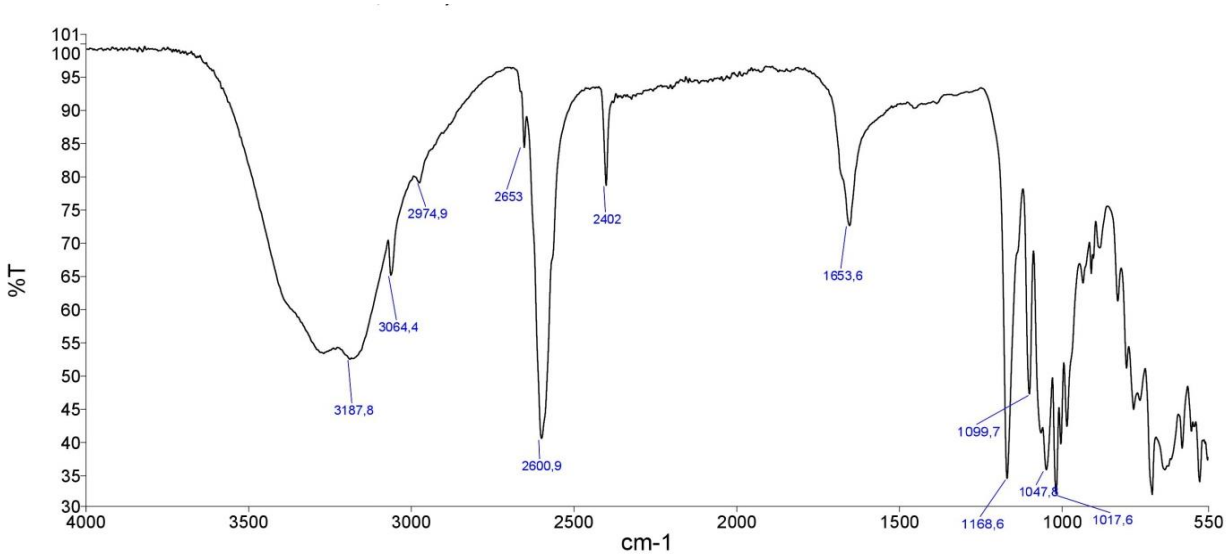

b)

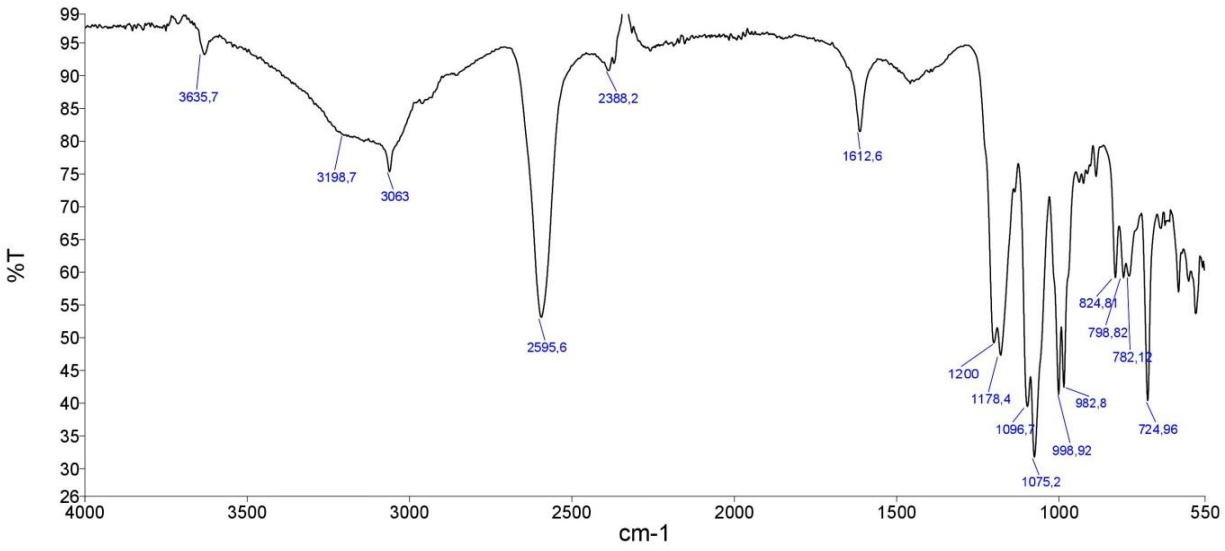

c)

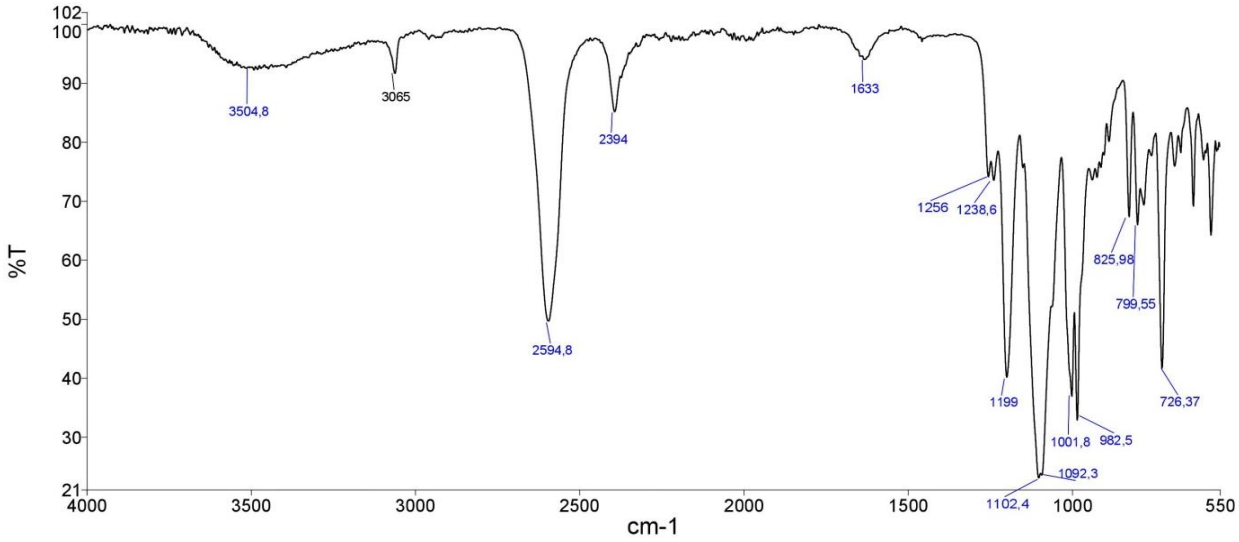
%T
cm-1
3504,8
3065
2394
1633
1256
1238,6
2594,8
1199
825,98
799,55
726,37
1001,8
982,5
1092,3
1102,4

d)

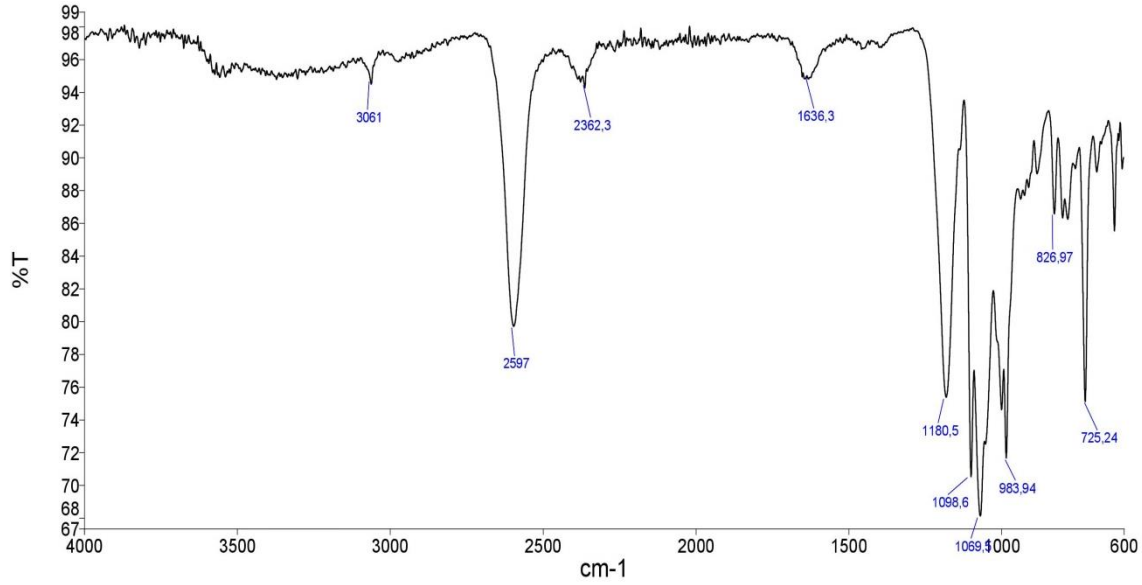
%T
cm-1
3061
2362,3
1636,3
826,97
2597
1180,5
725,24
1098,6
983,94

e)

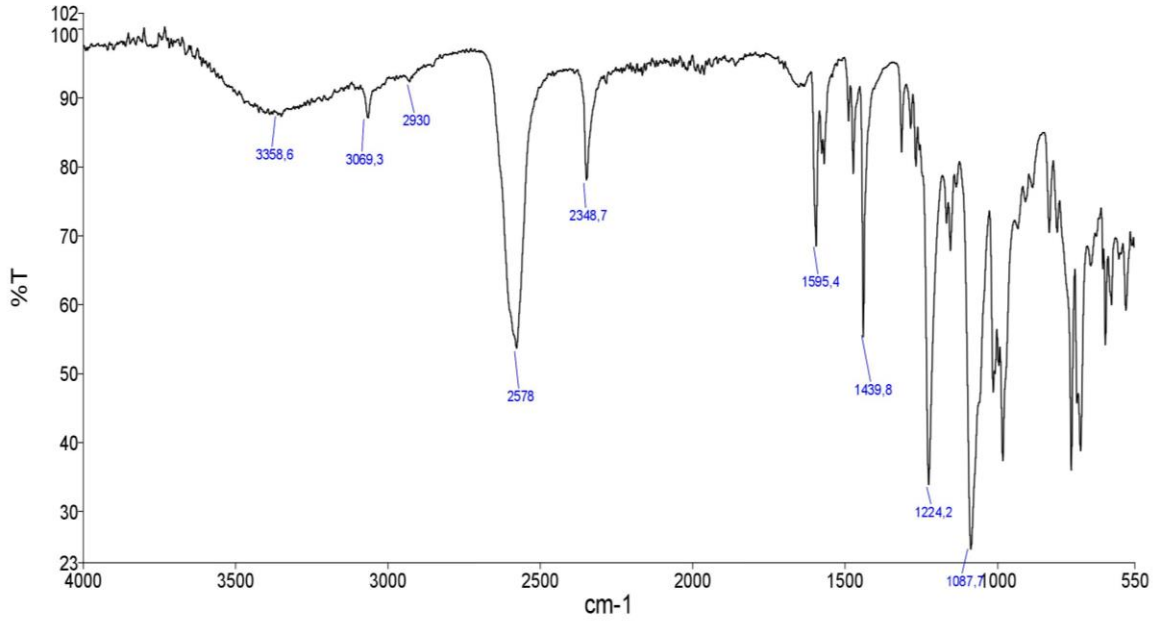
%T
cm-1
3358,6
3069,3
2930
2578
2348,7
1595,4
1439,8
1224,2
1087,7

f)

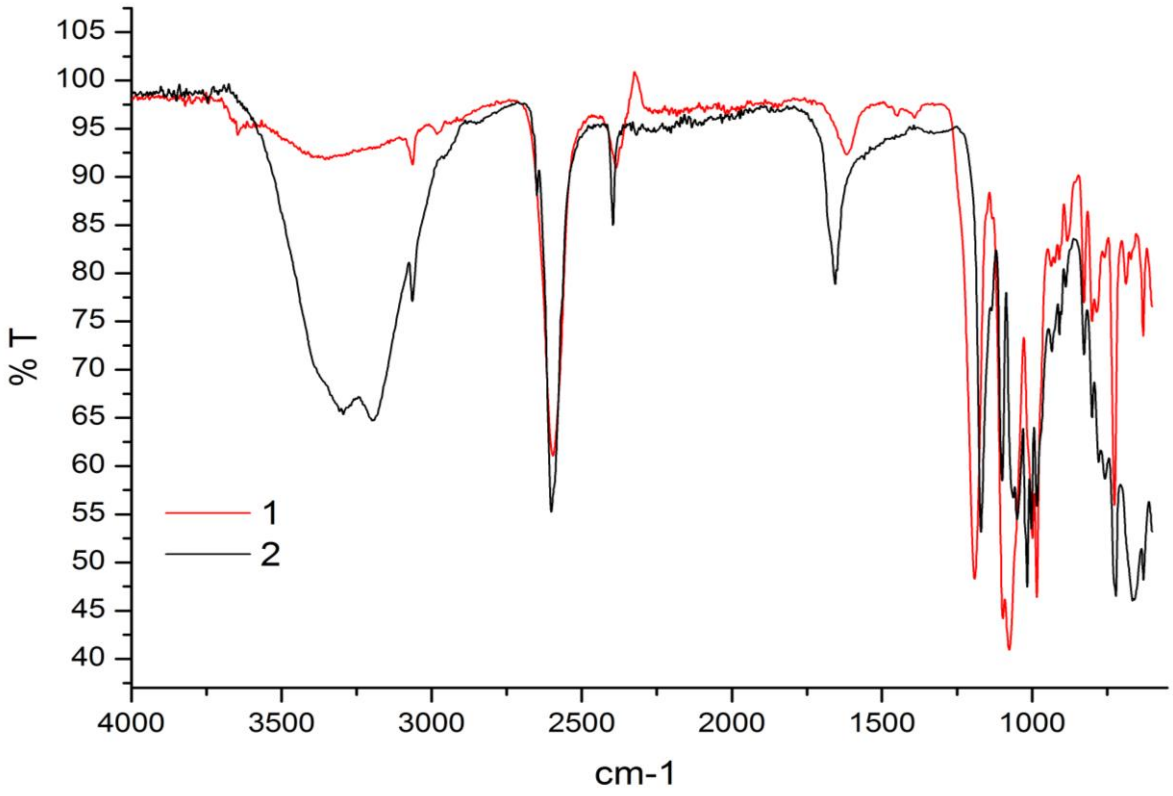
% T
cm-1
1
2

g)

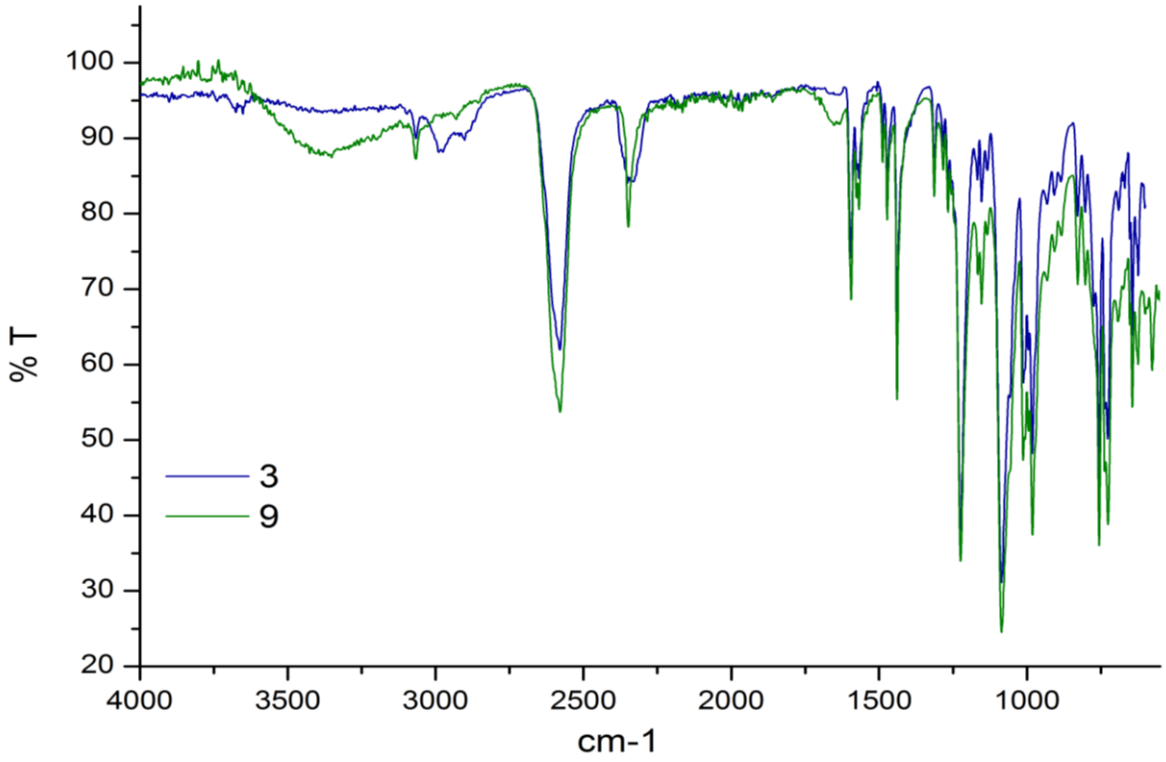
100
90
80
70
60
50
40
30
20
% T
3
9
4000
3500
3000
2500
2000
1500
1000
cm-1

h)

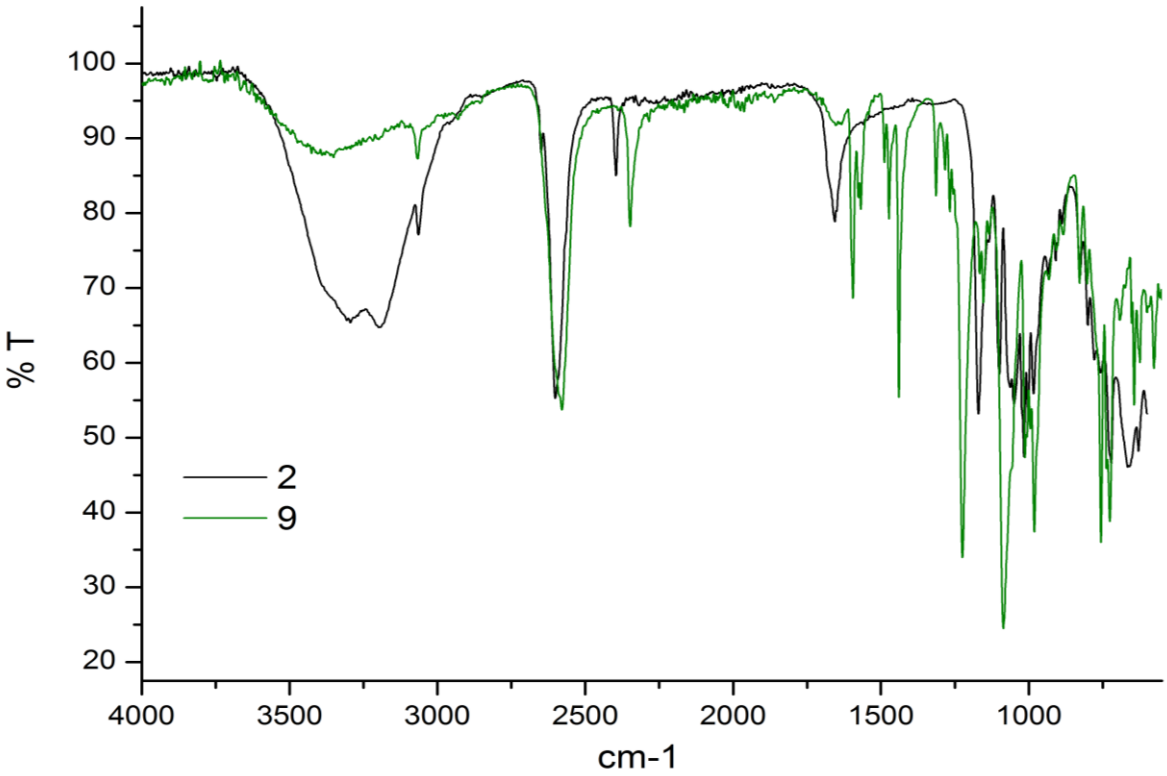
100
90
80
70
60
50
40
30
20
% T
2
9
4000
3500
3000
2500
2000
1500
1000
cm-1

Figure S2. ^{11}B-NMR and ^{11}B{^{1}H}-NMR spectra of the compound **4**

^{11}B-NMR

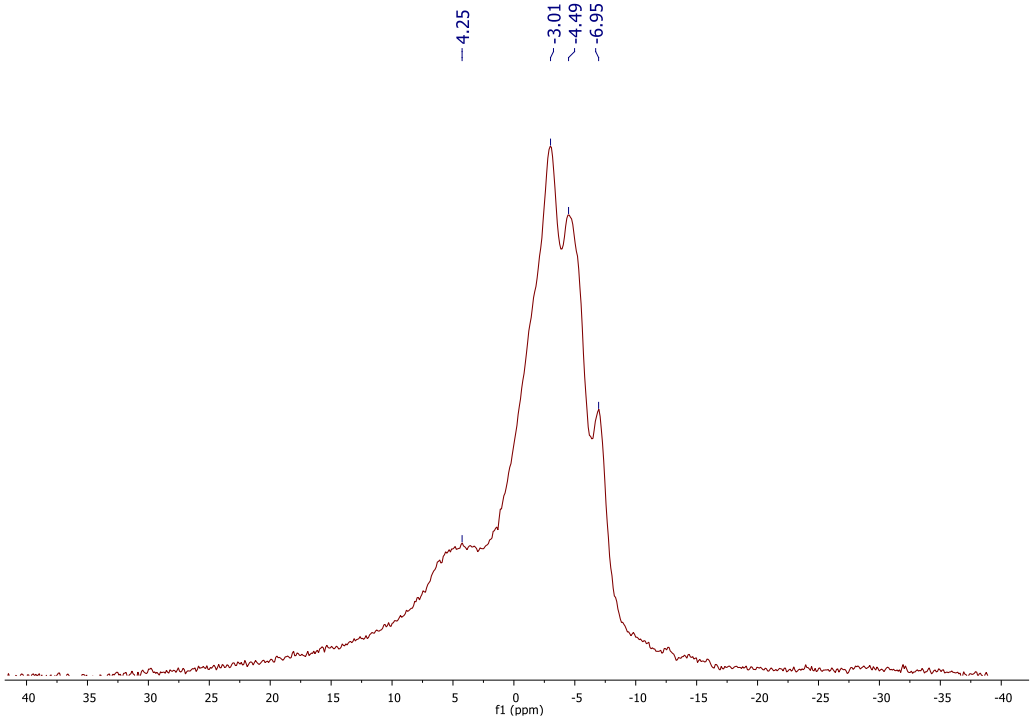

^{11}B{^{1}H}-NMR

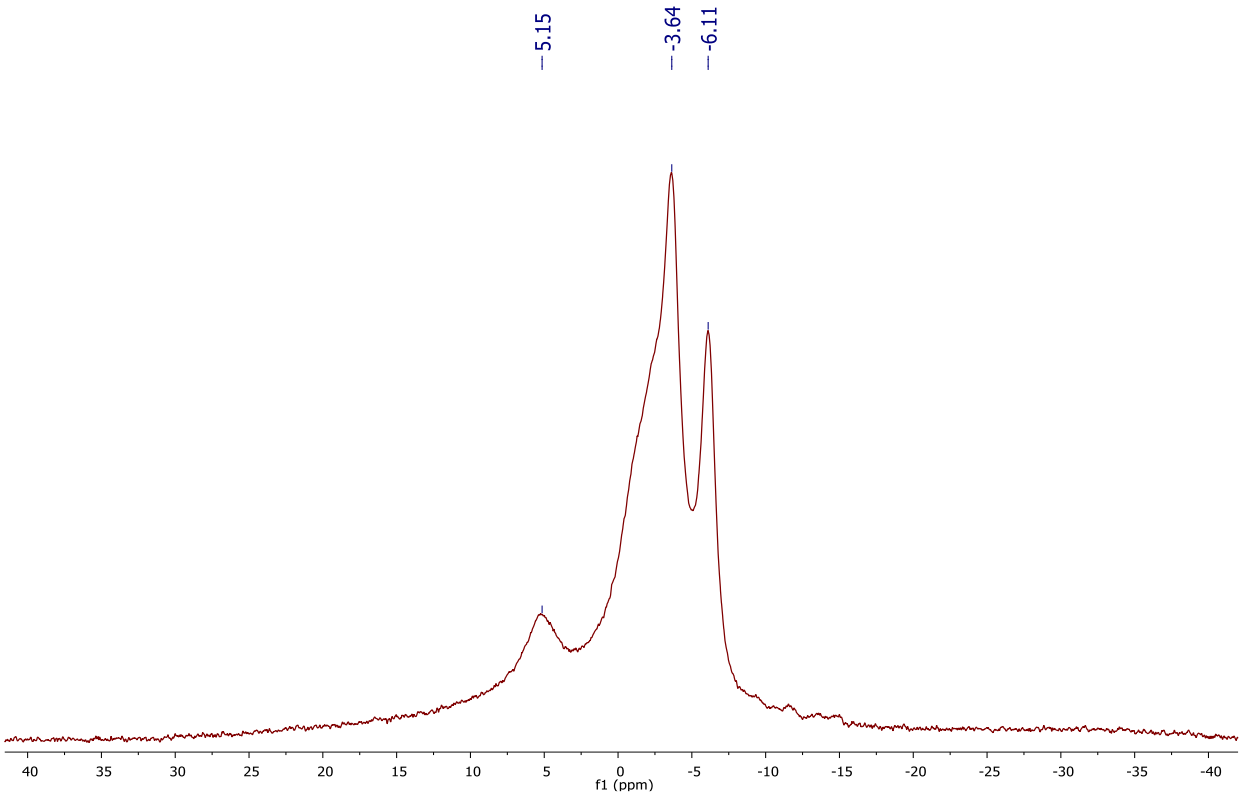

Figure S3. ^{11}B-NMR and ^{11}B{^{1}H}-NMR spectra of the compound **6**

^{11}B-NMR

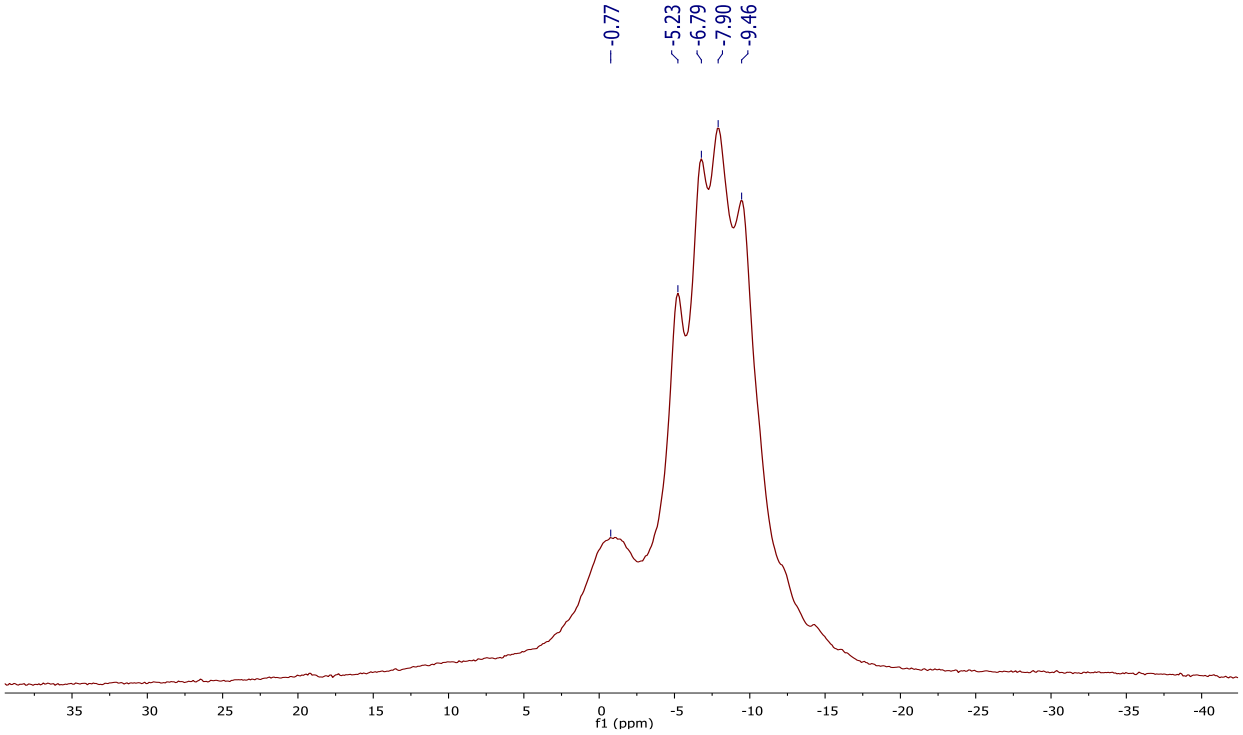

^{11}B{^{1}H}-NMR

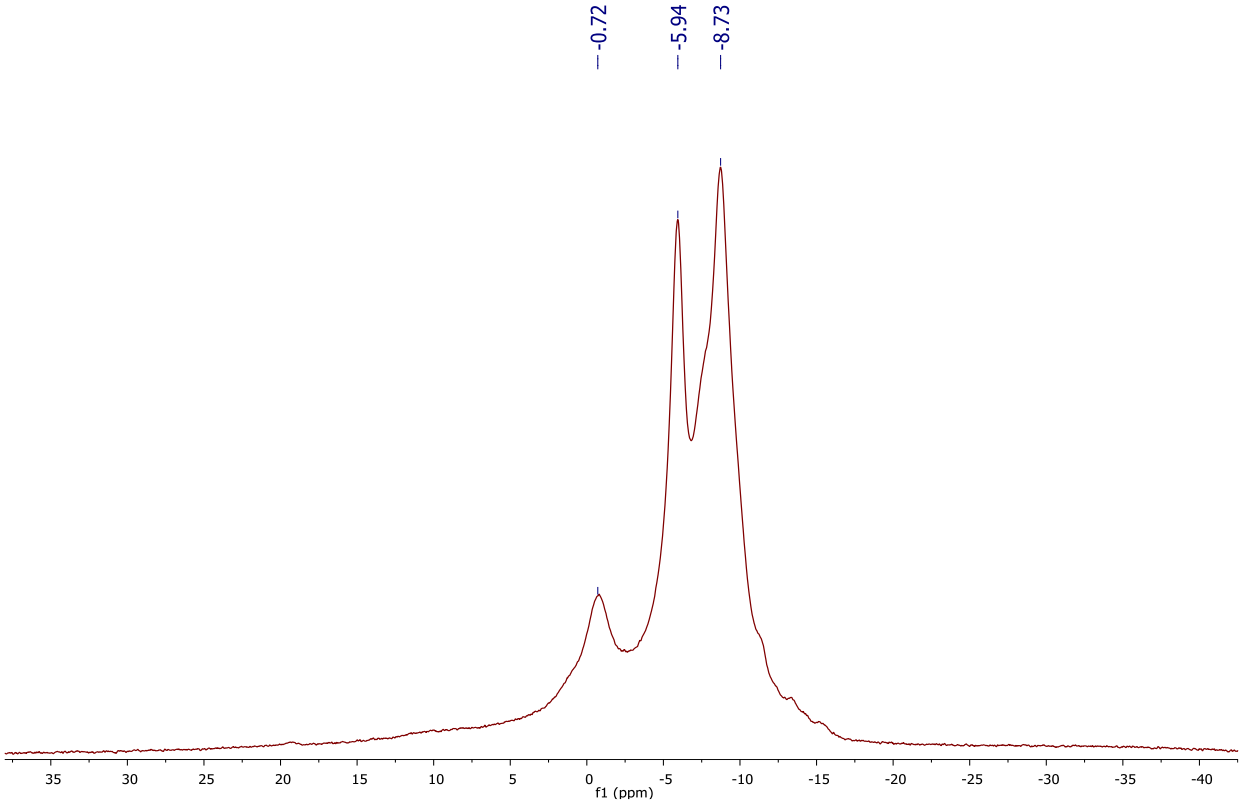

Figure S4. ^{1}H-NMR, ^{1}H{^{11}B}-NMR, ^{11}B-NMR, ^{11}B{^{1}H}-NMR, ^{31}P-NMR, ^{13}C{^{1}H}-NMR spectra of the compound **7**.

^{1}H-NMR

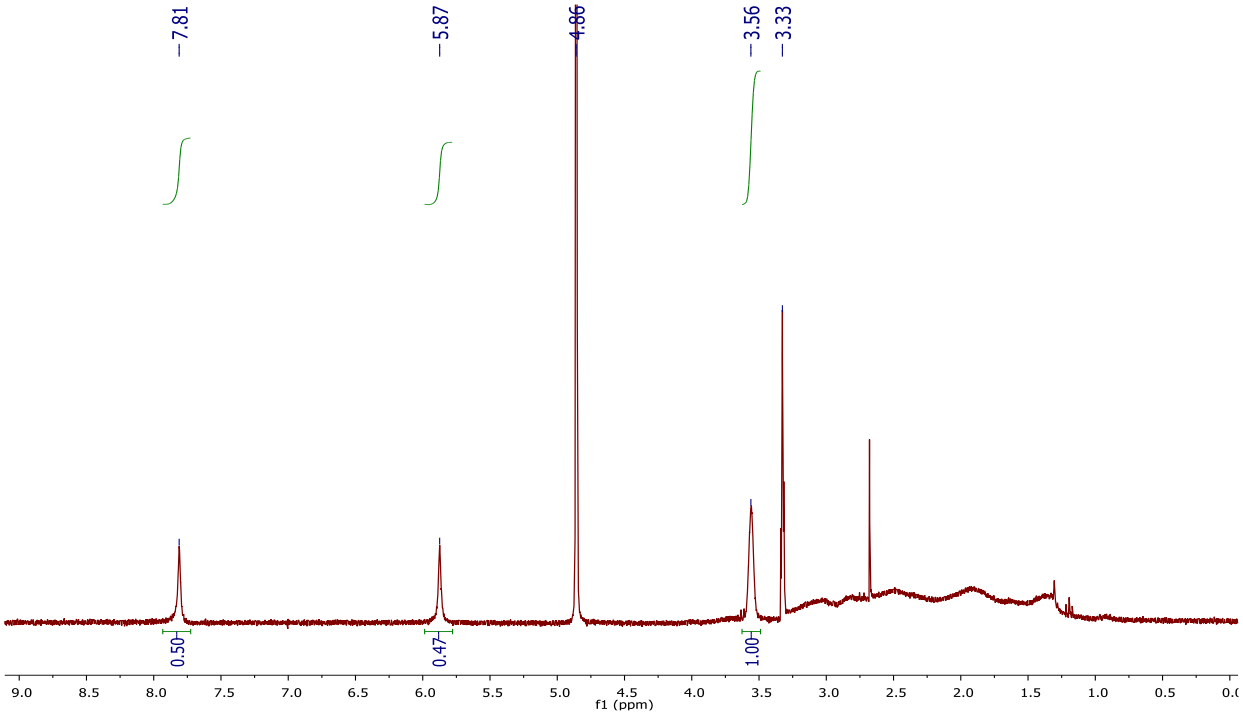

^{1}H{^{11}B}-NMR

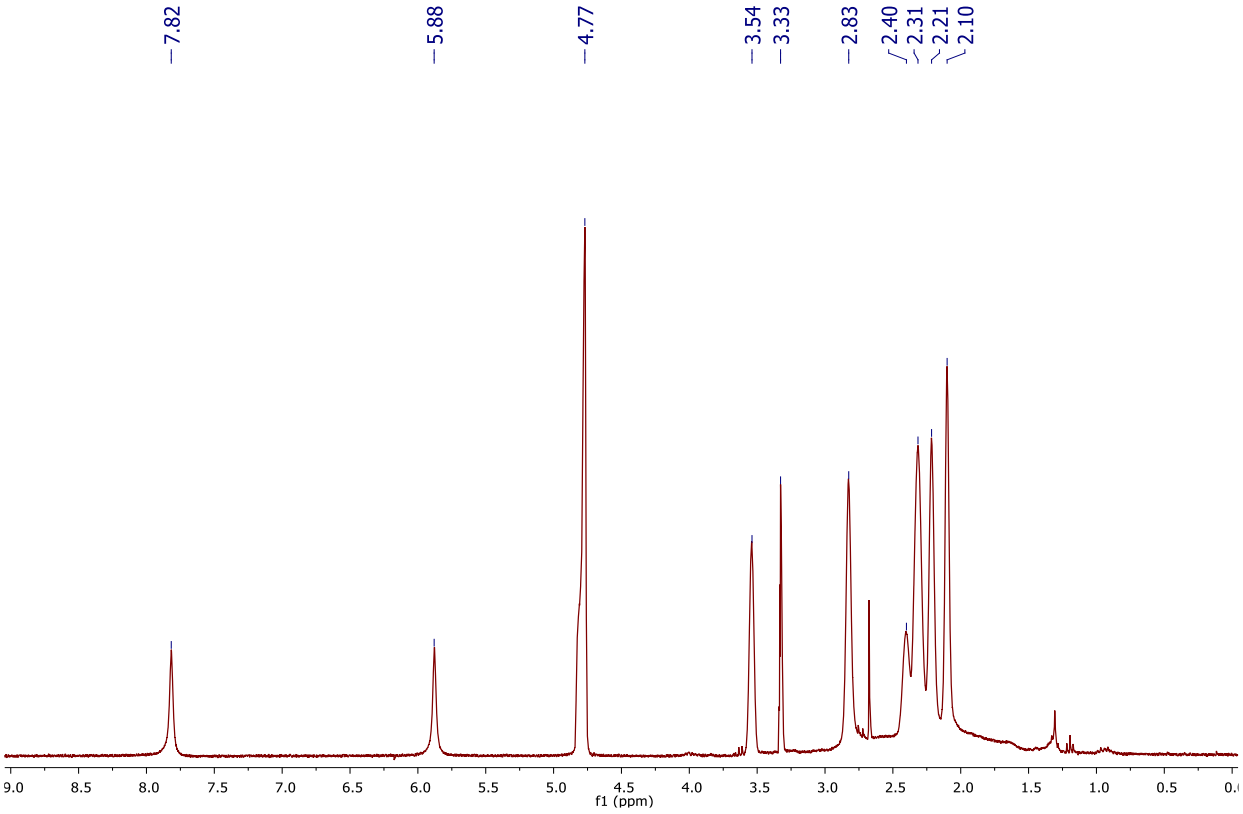

^{11}B-NMR

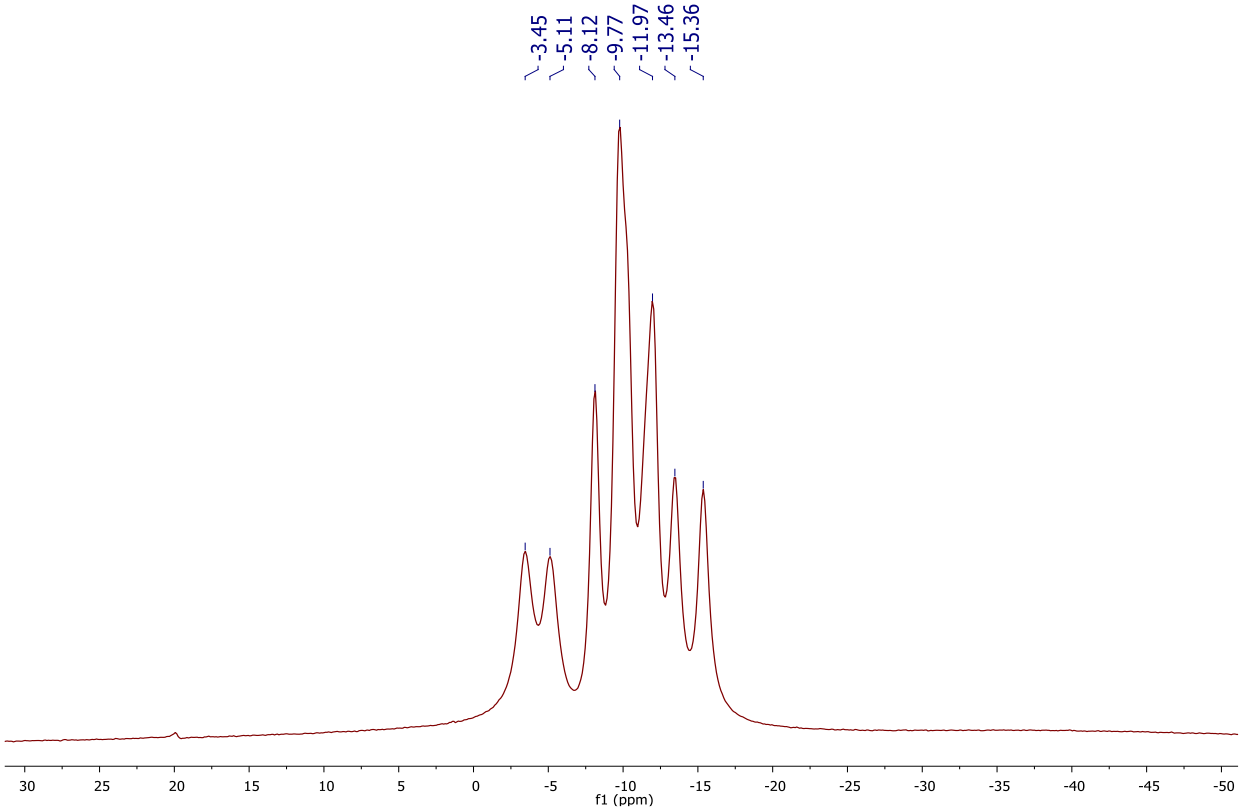

^{11}B{^{1}H}-NMR

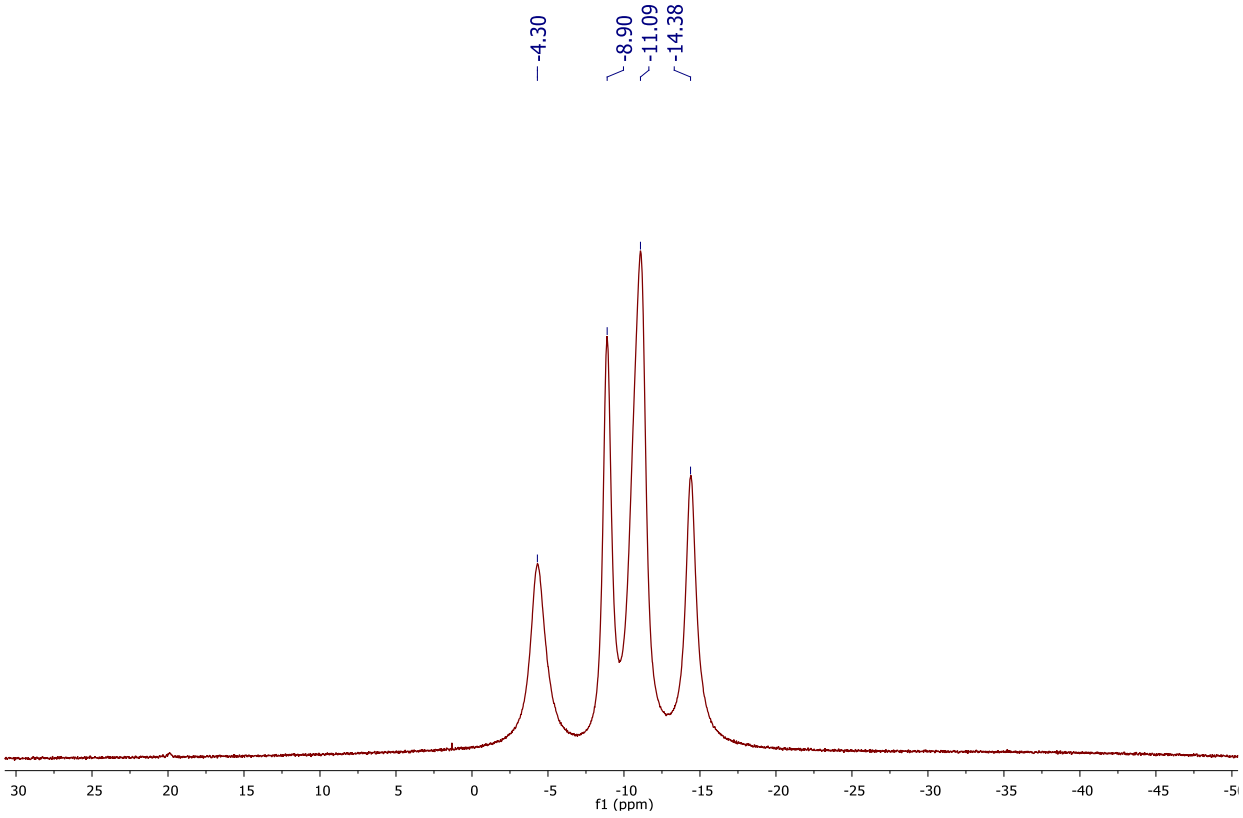

^{31}P-NMR

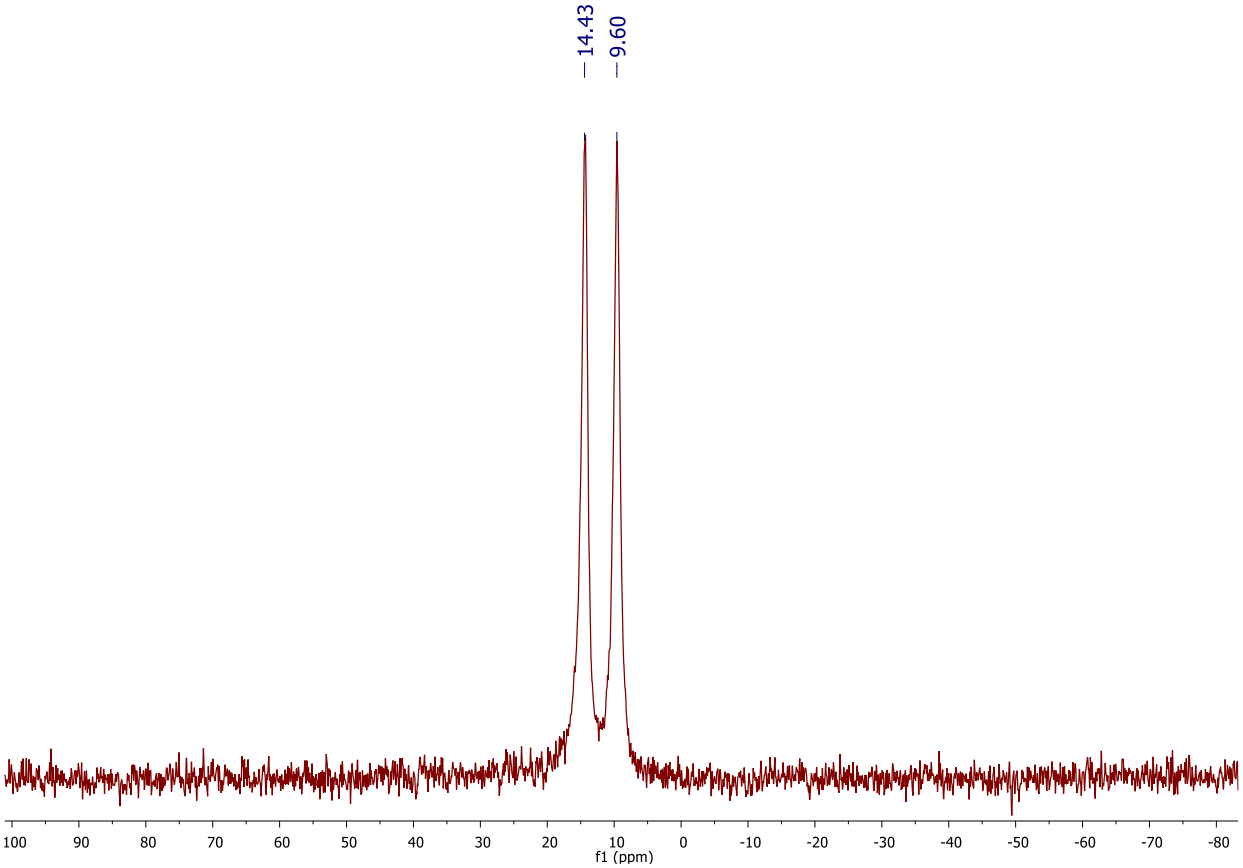

^{13}C{^{1}H}-NMR

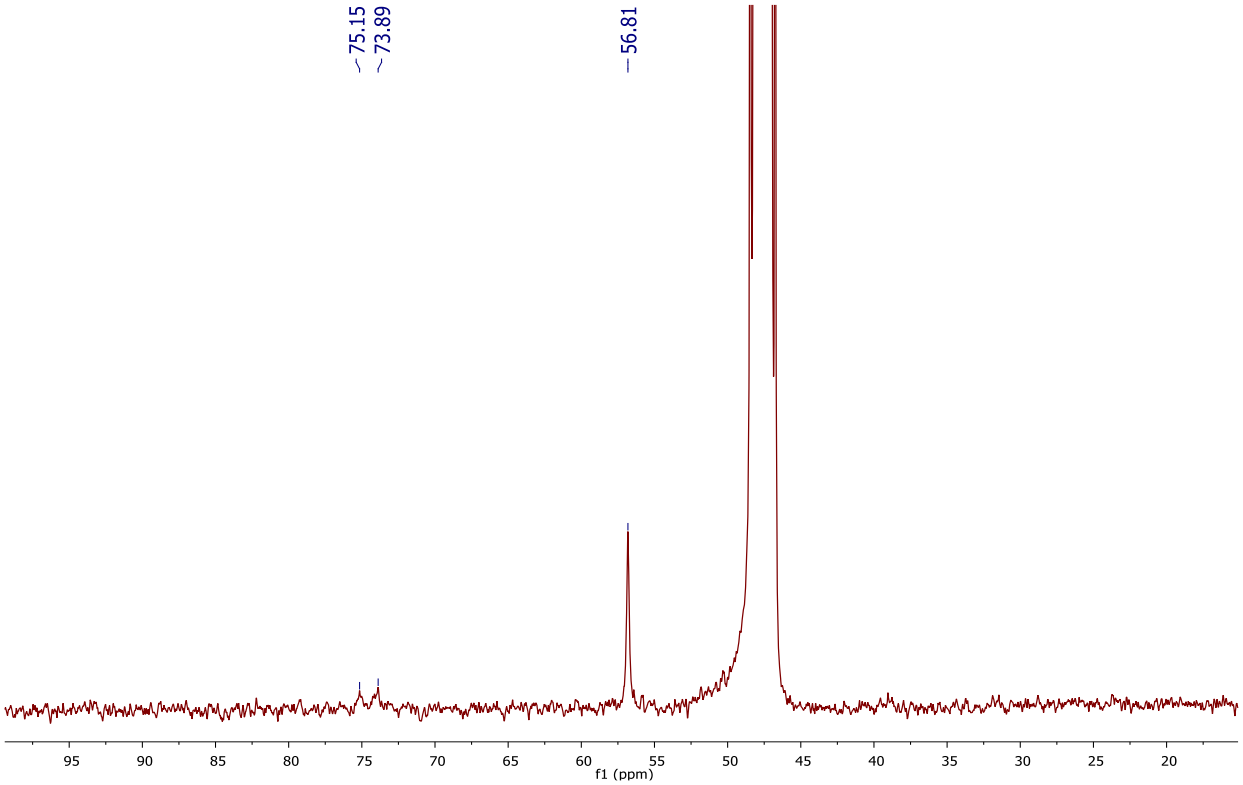

Figure S5. ^{1}H-NMR, ^{1}H{^{11}B}-NMR, ^{11}B-NMR, ^{11}B{^{1}H}-NMR, ^{31}P-NMR, ^{13}C{^{1}H}-NMR spectra of the compound **8**.

^{1}H-NMR

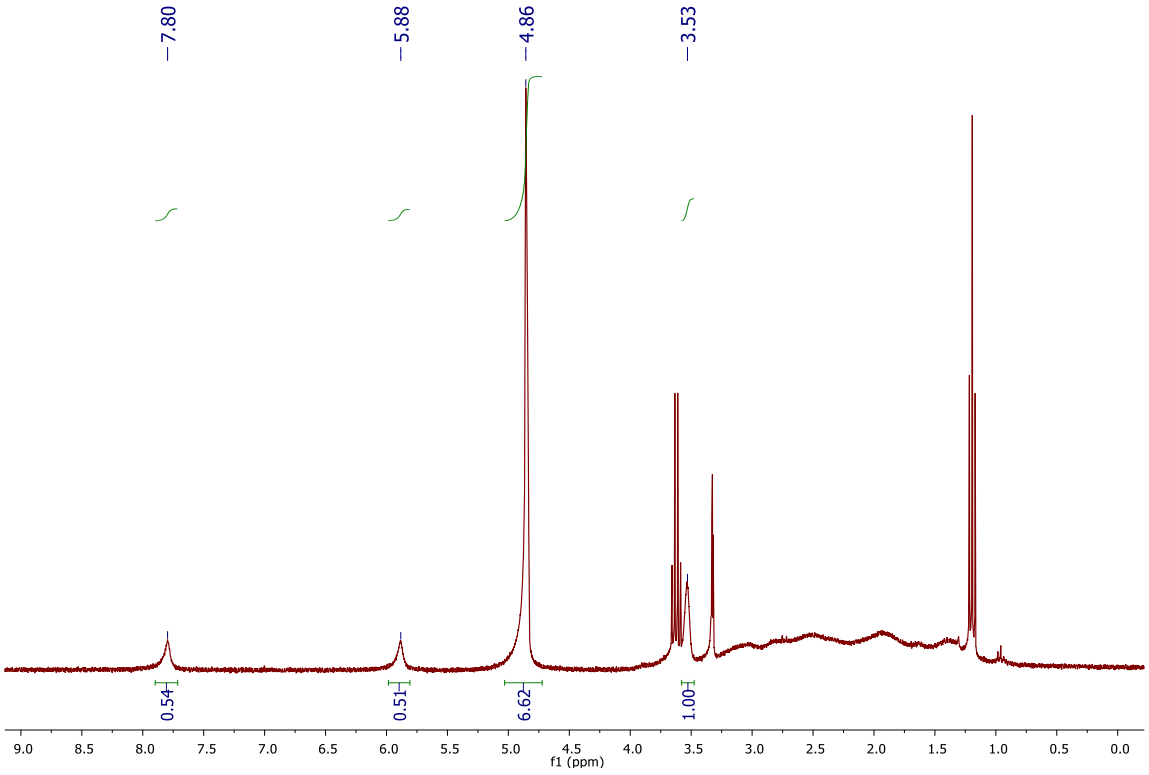

^{1}H{^{11}B}-NMR

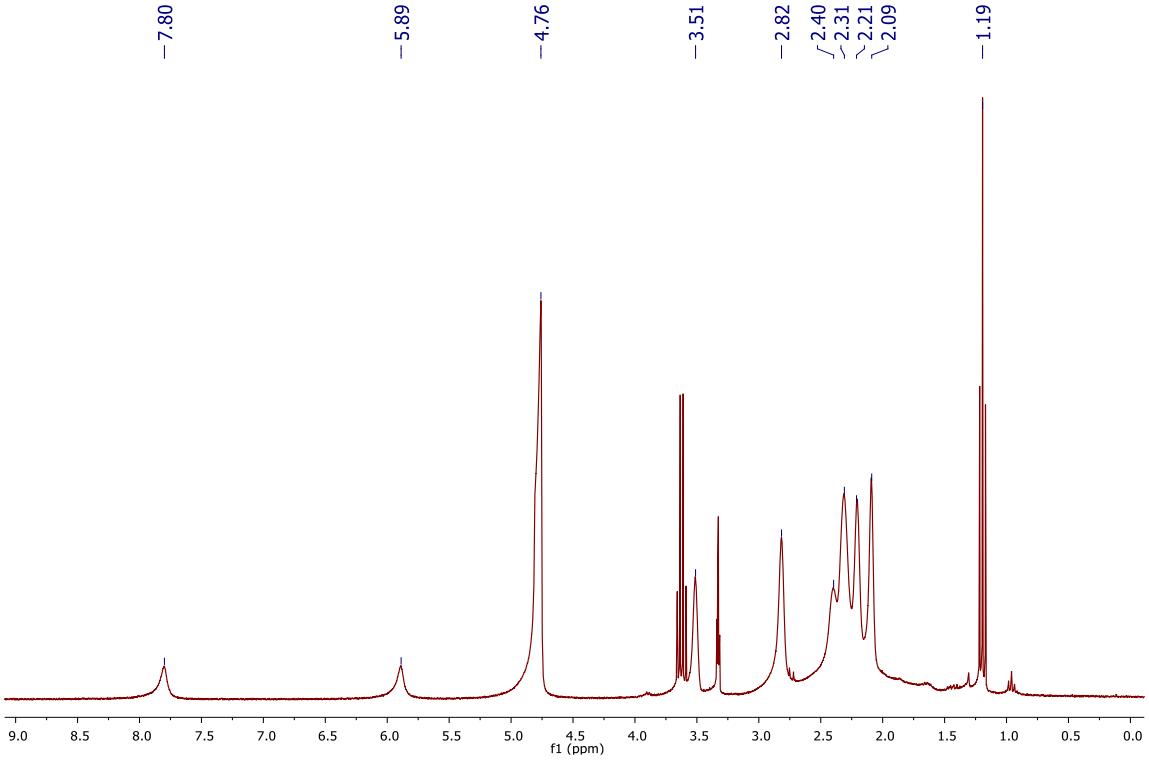

^{11}B-NMR

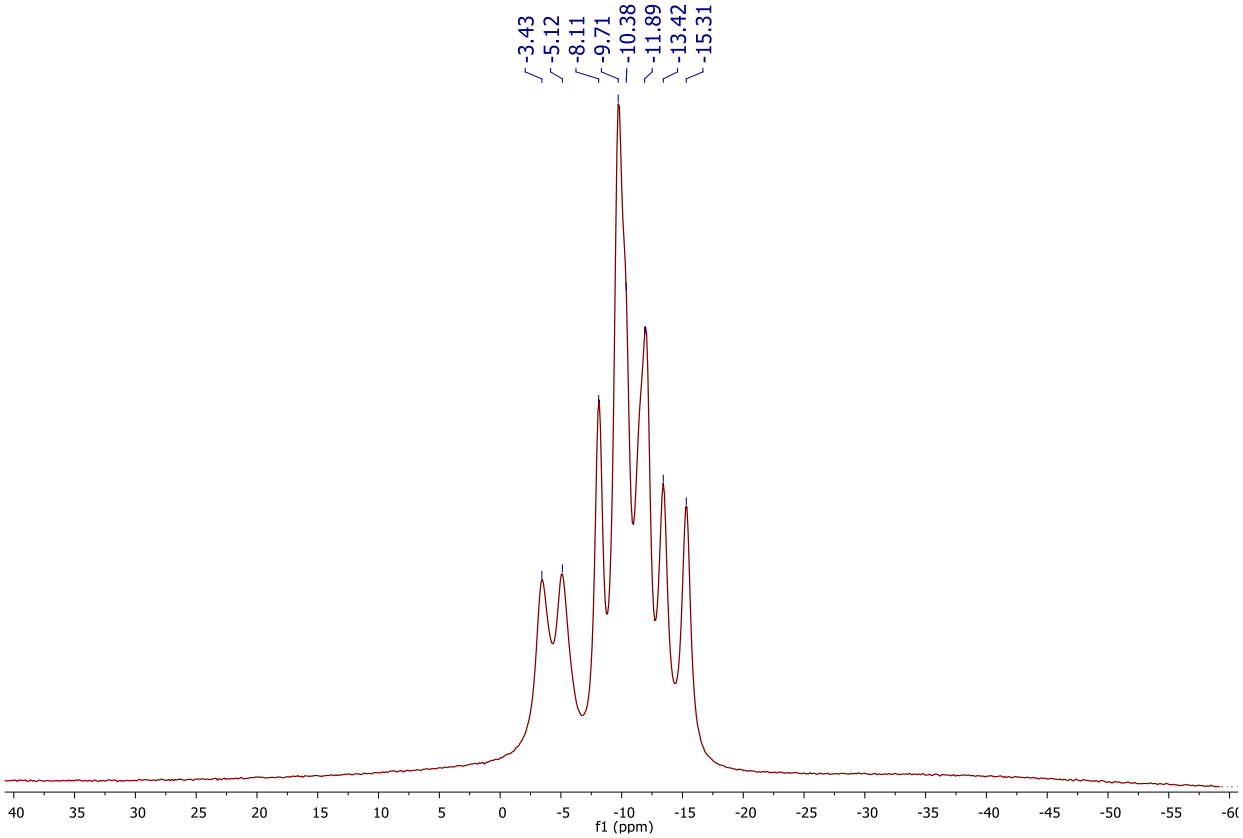

^{11}B{^{1}H}-NMR

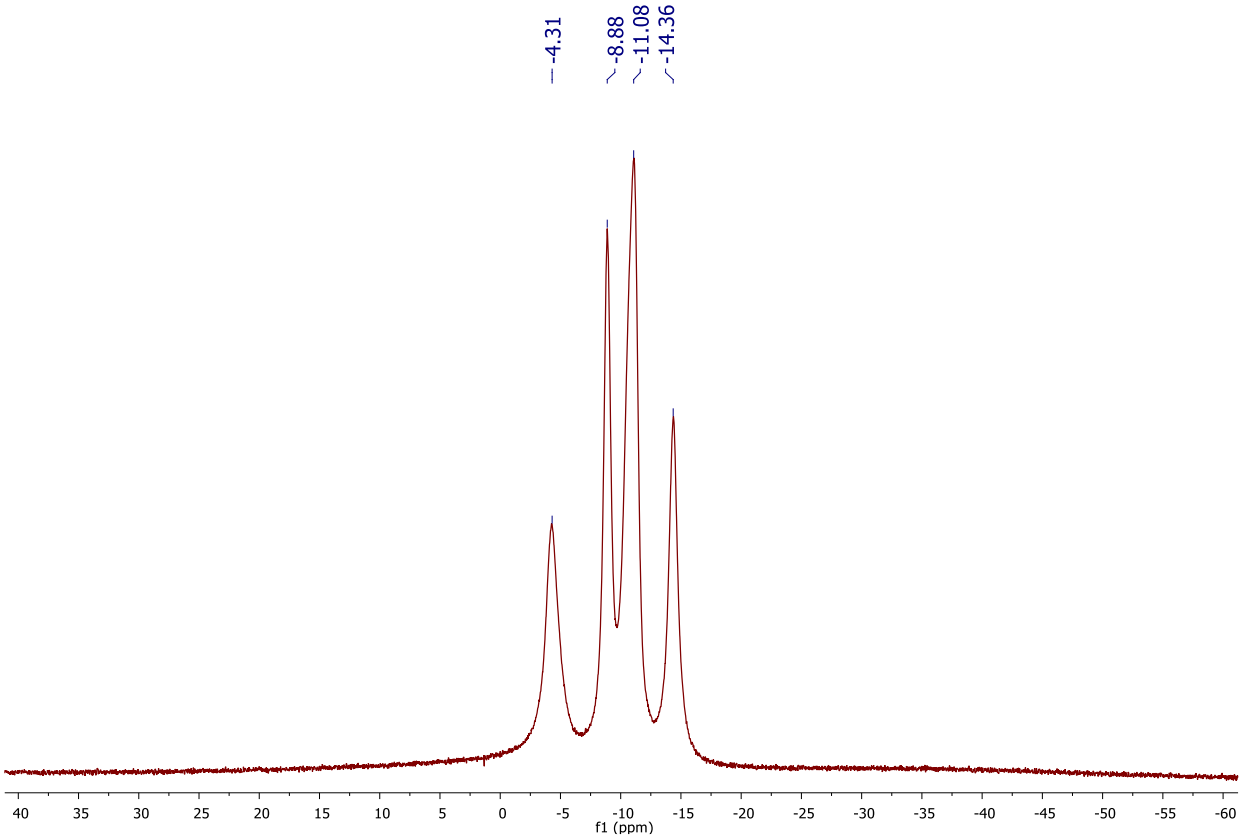

^{31}P-NMR

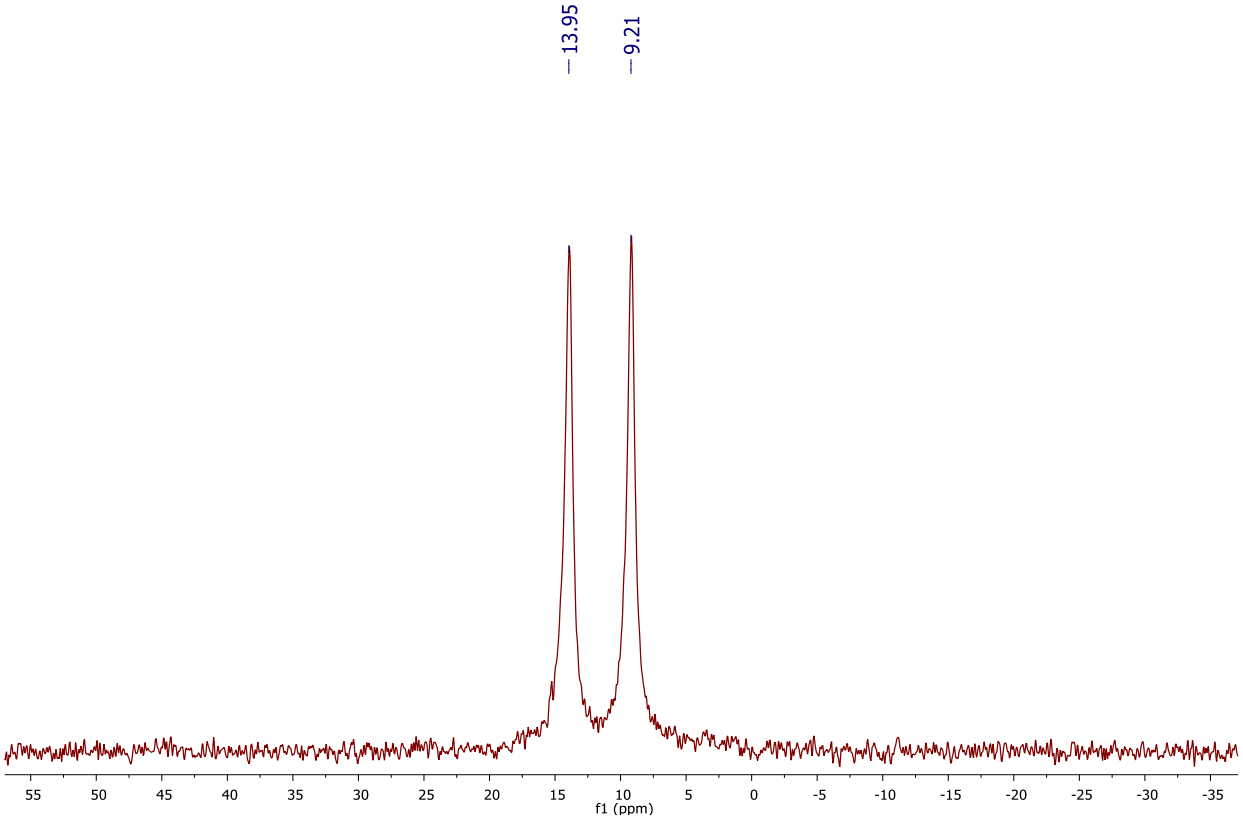

^{13}C{^{1}H}-NMR

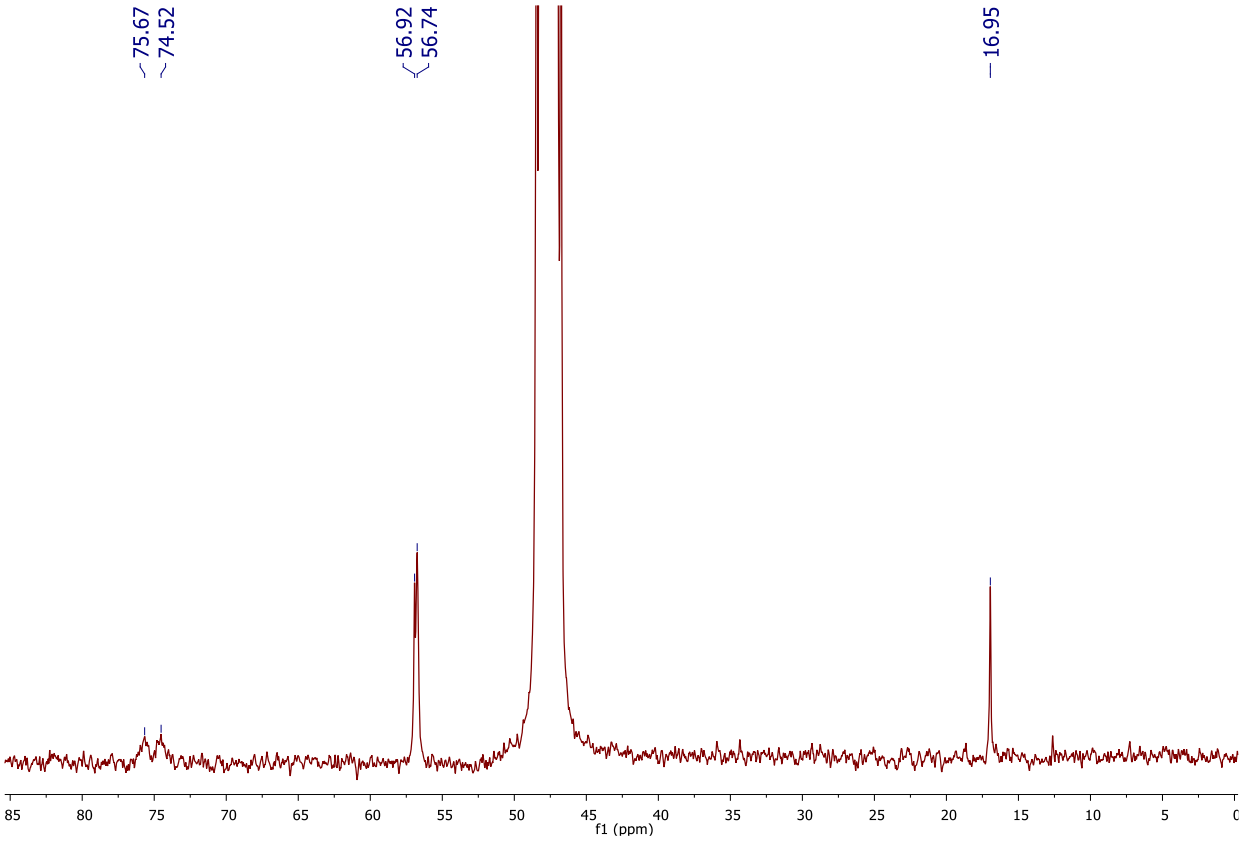

Figure S6. ^{11}B-NMR and ^{11}B{^{1}H}-NMR spectra of the compound **9**.

^{11}B-NMR

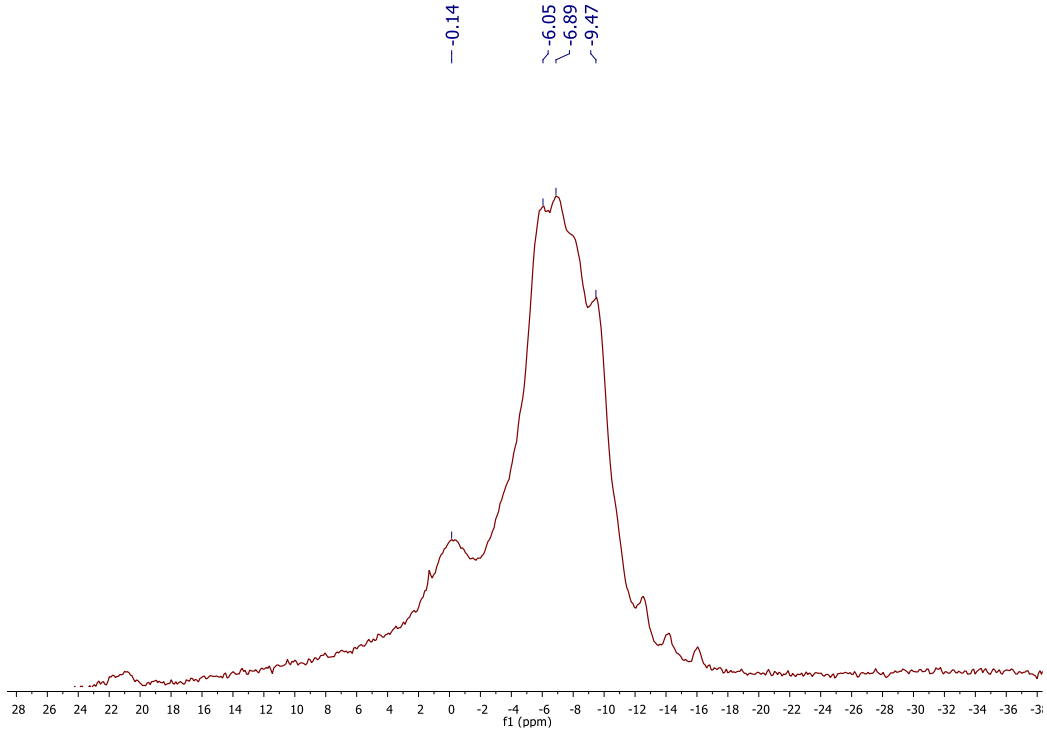

^{11}B{^{1}H}-NMR

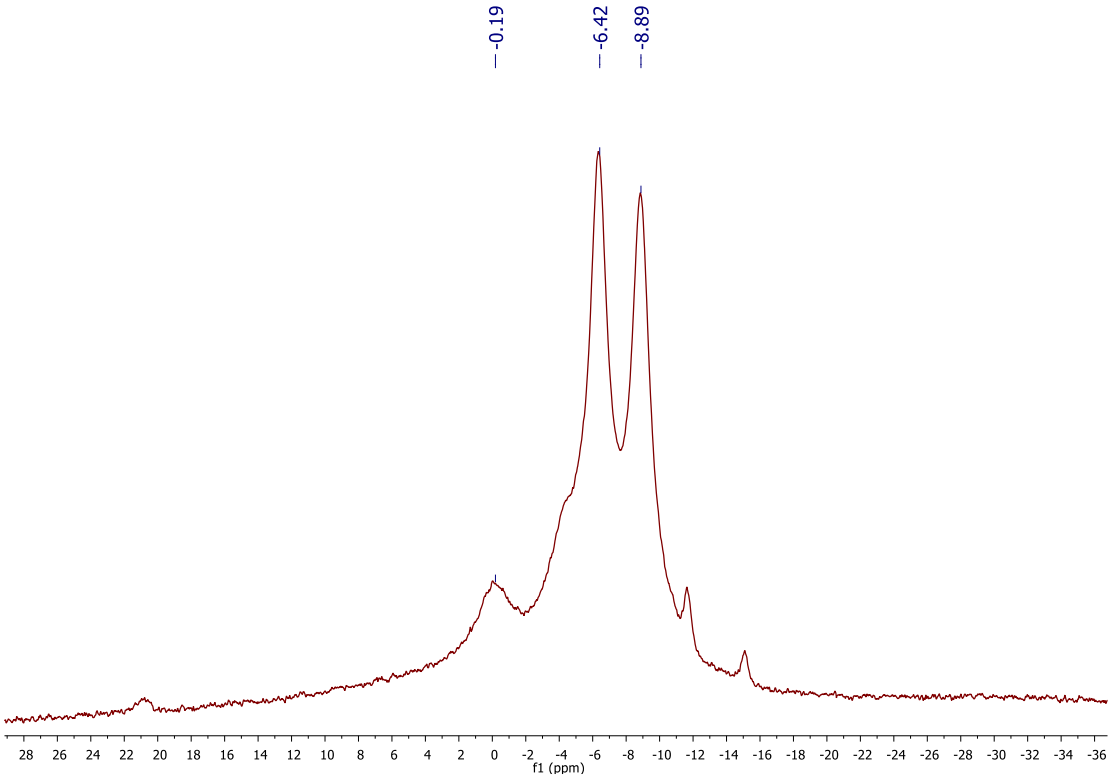

Figure S7. Evolution of the $^{11}B\{^1H\}$-NMR spectrum of compound **3** in MeOH/H_2O to produce lower nuclearity species as compound **2**.

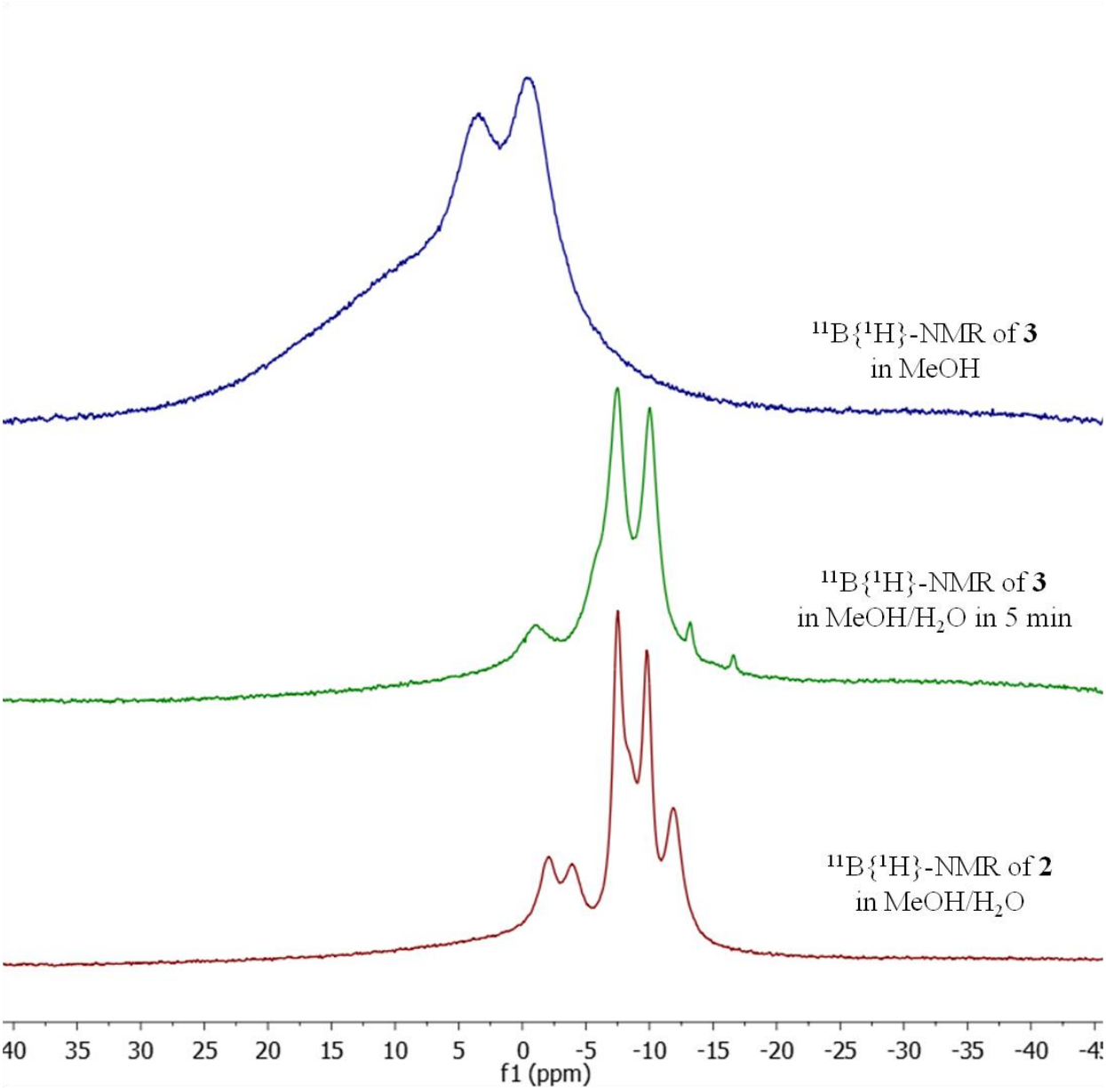

Figure S8. Packing structure of Cd polymer **8.**

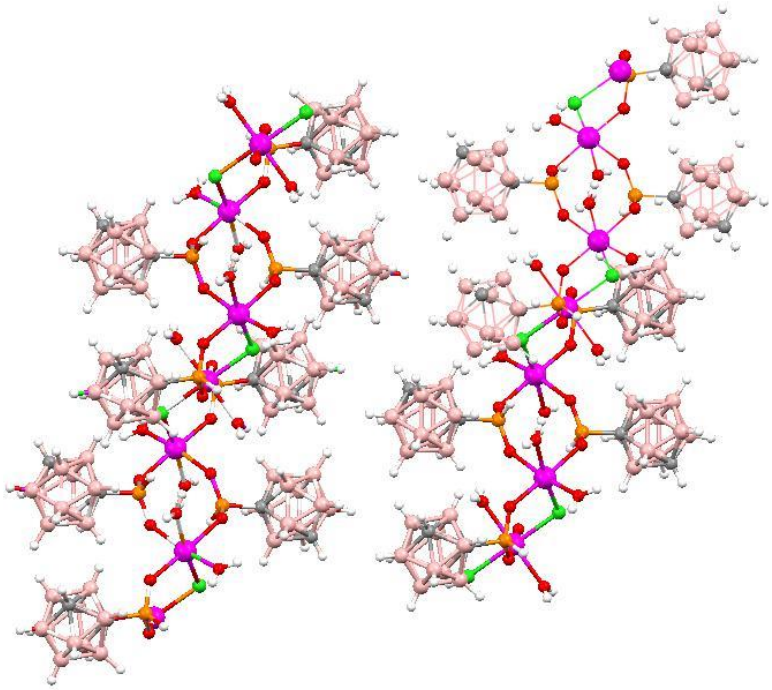

Figure S9. X-ray powder diffraction (XRPD) of **6** (a) (Cu complex) and **7** (b) (Zn complex)

a)

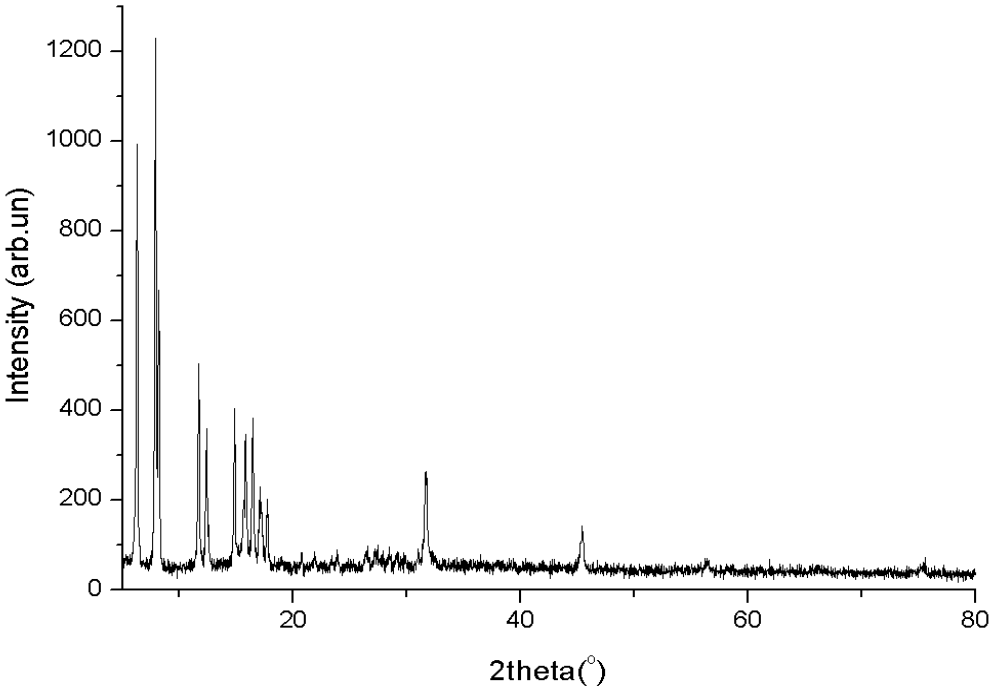

b)

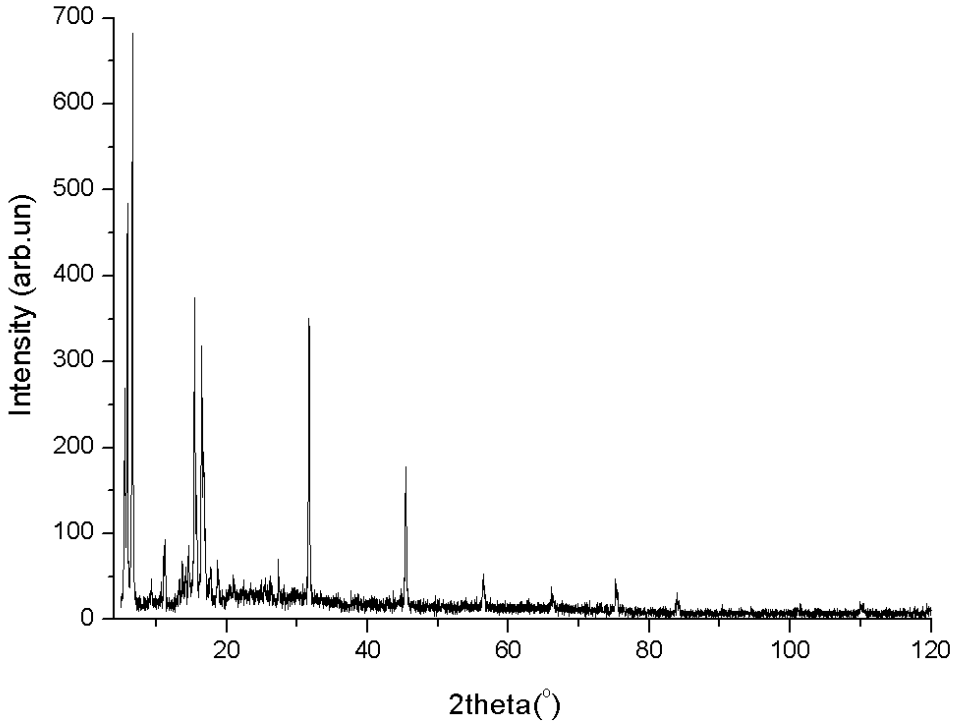

Figure S10. Thermal gravimetric analysis (TGA/DCS) of a) **6**; b) **7** and c) **8**.

a)

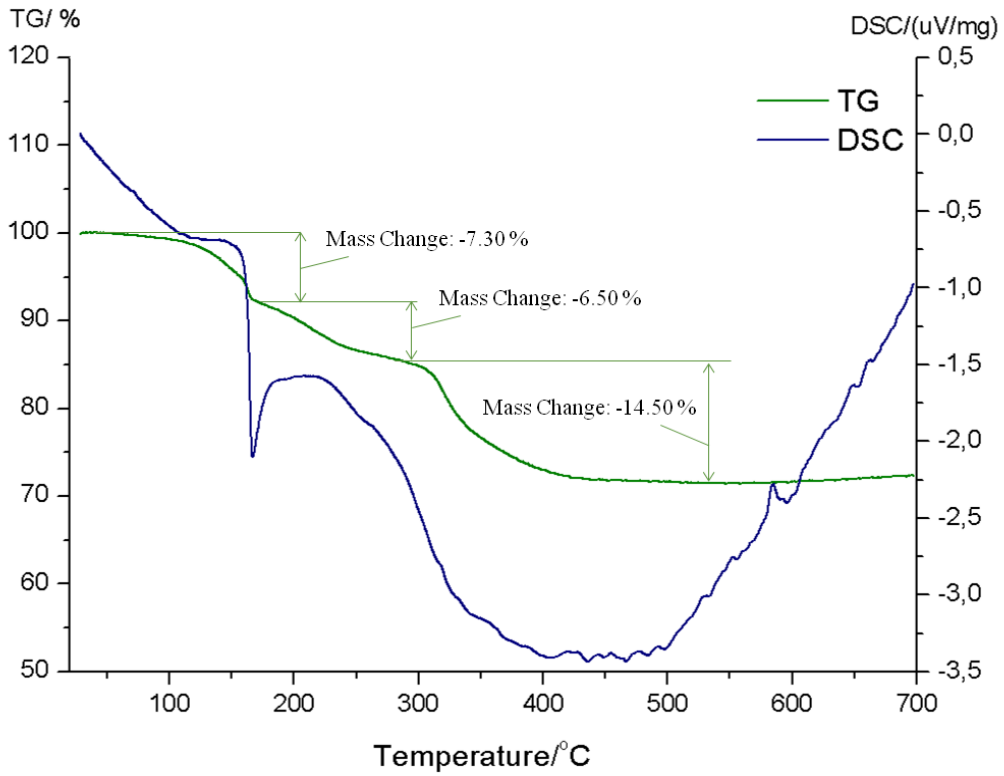

b)

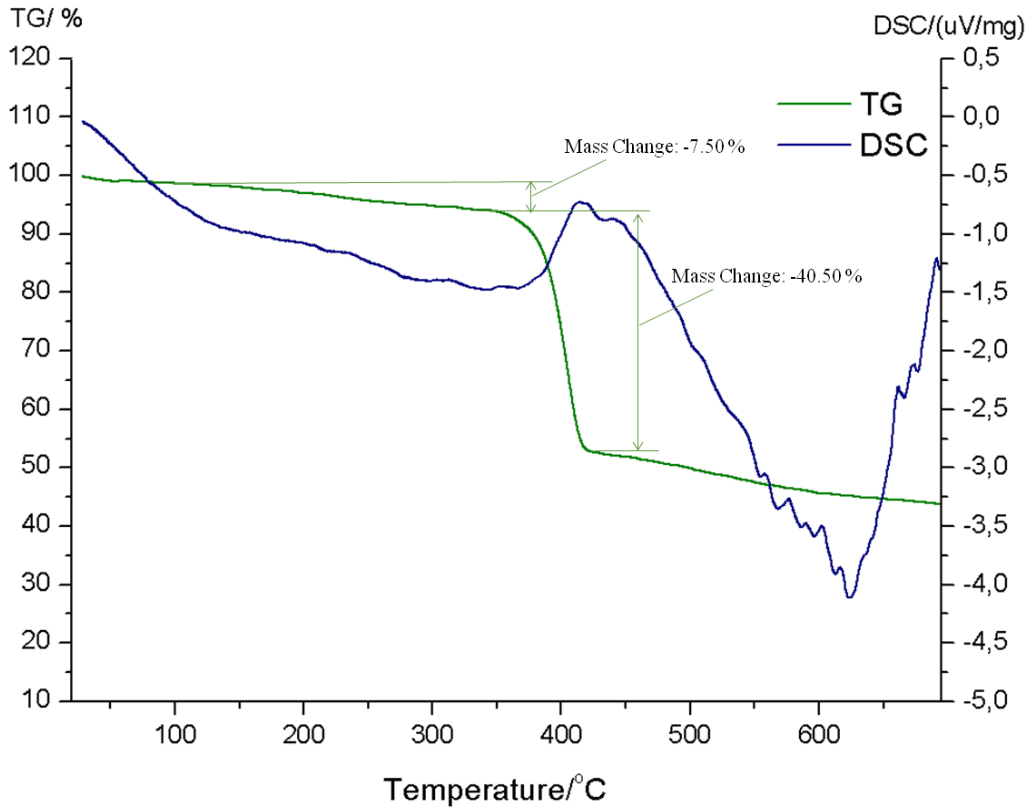

c)

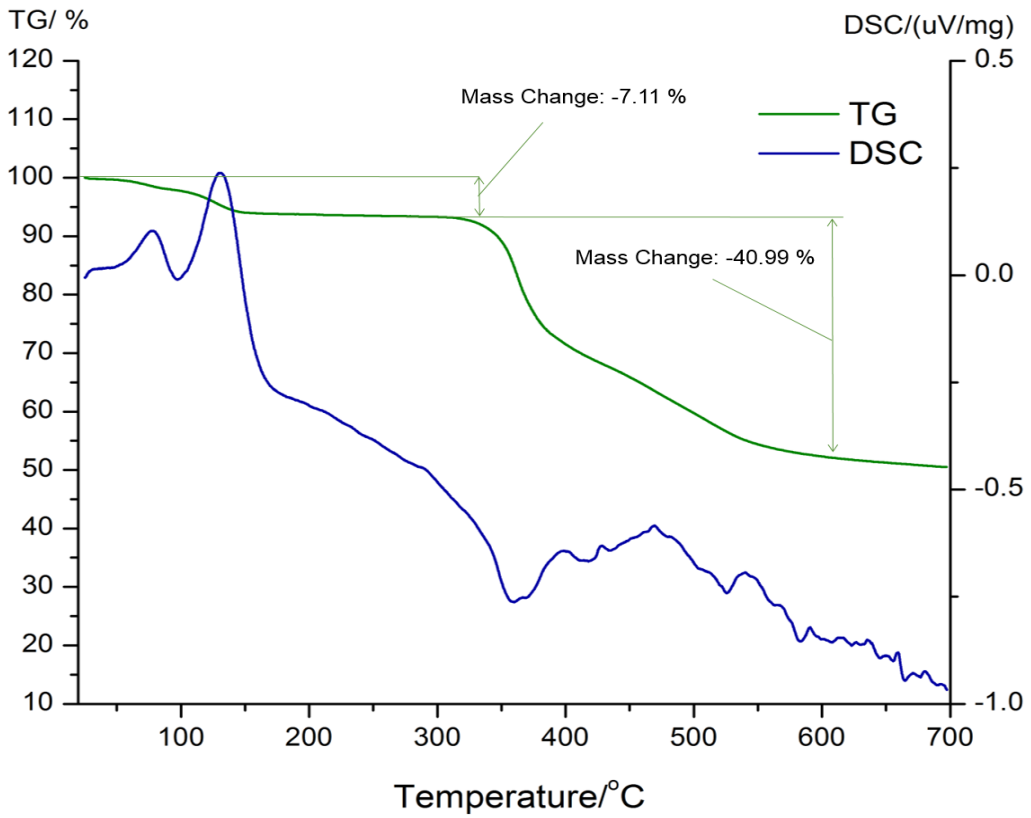
TG/ %
DSC/(uV/mg)
Mass Change: -7.11 %
Mass Change: -40.99 %
TG
DSC
120
110
100
90
80
70
60
50
40
30
20
10
0.5
0.0
-0.5
-1.0
100
200
300
400
500
600
700
Temperature/°C

Figure S11. EPR of a) coordination polymer **1**, b) **2** and c) coordination polymer **3** at different temperatures on powder samples.

a)

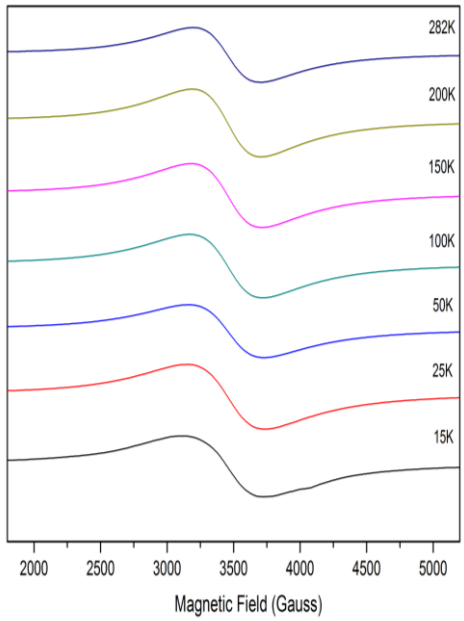

b)

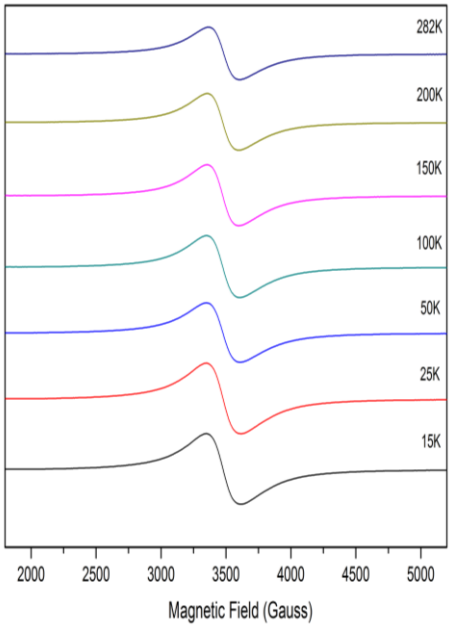

c)

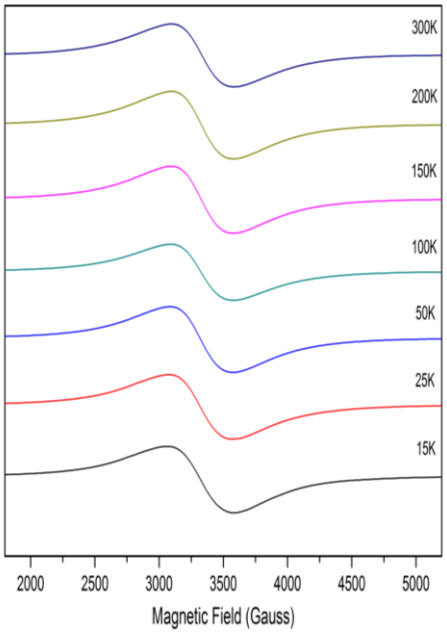

Table S1. Crystal Data for X-ray structures of Co complex, **4**.

	4
Empirical formula	$C_4H_{36}B_{20}CoO_{10}P_2$
Formula weight	581.42
Crystal system	Monoclinic
Space group	*C2/m*
a [Å]	11.184(2)
b [Å]	7.435(15)
c [Å]	17.041(3)
α [º]	90
β [º]	91.21(3)
γ [º]	90
V [Å^3]	1416.7(5)
Formula Units/Cell	2
$\rho_{calc.}$ [g cm^{-3}]	1.335
μ [mm^{-1}]	1.036
$R1$[a], [I > 2σ(I)]	0.0868
wR_2[b] [all data]	0.2473

[a] $R_1 = \Sigma||F_o| - |F_c||/\Sigma|F_o|$

[b] $wR_2 = [\Sigma\{w(F_o^2-F_c^2)^2\}/\Sigma\{w(F_o^2)^2\}]^{½}$, where $w=1/[\sigma^2(Fo^2)+(0.0042P)^2]$ and $P=(F_o^2+2F_c^2)/3$

Table S2. Selected bond lengths (Å) and angles (°) for Co complex, **4**.

	4
Co(1)-O(3)	2.103(3)
Co(1)-O(3)#1	2.103(3)
Co(1)-O(3)#2	2.103(3)
Co(1)-O(2)#3	2.103(3)
Co(1)-O(2)	2.078(4)
Co(1)-O(2)#2	2.079(4)
O(2)-Co(1)-O(2)#2	180.00
O(2)-Co(1)-O(3)	86.97(10)
O(2)#2-Co(1)-O(3)	93.03(10)
O(2)-Co(1)-O(3)#1	86.97(10)
O(2)#2-Co(1)-O(3)#1	93.03(10)
O(3)-Co(1)-O(3)#1	99.45(15)
O(2)-Co(1)-O(3)#3	93.03(10)
O(2)#2-Co(1)-O(3)#3	86.97(10)
O(3)-Co(1)-O(3)#3	80.55
O(3)#1-Co(1)-O(3)#3	180.00(17)
O(2)-Co(1)-O(3)#2	93.03(10)
O(2)#2-Co(1)-O(3)#2	86.97(10)
O(3)-Co(1)-O(3)#2	180.00
O(3)#1-Co(1)-O(3)#2	80.55(15)
O(3)#3-Co(1)-O(3)#2	99.45(15)

Symmetry transformations used to generate equivalent atoms:

#1 x,-y,z #2 -x+1,-y,-z #3 -x+1,y,-z

Table S3. Crystal Data for X-ray structures of Cd complex **8**.

	6
Empirical formula	$C_8H_{60}B_{40}Cd_3Cl_2O_{14}P_4$
Formula weight	1344.94
Crystal system	Triclinic
Space group	*P-1*
a [Å]	7.3508(18)
b [Å]	10.847(3)
c [Å]	16.600(4)
α [º]	106.839(4)
β [º]	95.487(4)
γ [º]	92.549(4)
V [Å^3]	1257.4(6)
Formula Units/Cell	1
$\rho_{calc.}$ [g cm^{-3}]	1.760
μ [mm^{-1}]	1.542
$R1$[a], [I > 2σ(I)]	0.0526
wR_2[b] [all data]	0.1391

[a] $R_1 = \Sigma||F_o| - |F_c||/\Sigma|F_o|$

[b] $wR_2 = [\Sigma\{w(F_o^2-F_c^2)^2\}/\Sigma\{w(F_o^2)^2\}]^{½}$,where $w = 1/[\sigma^2(Fo^2) + (0.0042P)^2]$ and $P=(F_o^2+2F_c^2)/3$

Table S4. Selected bond lengths (Å) and angles (°) for Cd complex **8**.

Cd(1)-Cl(4)	2.5310(11)	O(1)-Cd(1)-O(5)#1	96.43(9)
Cd(1)-O(1)	2.327(2)	Cl(4)#1-Cd(1)-O(5)	89.92(8)
Cd(1)-O(5)	2.330(3)	O(1)#1-Cd(1)-O(5)	96.43(9)
Cd(1)-Cl(4)#1	2.5310(11)	O(5)-Cd(1)-O(5)#1	180.00
Cd(1)-O(1)#1	2.327(2)	Cl(4)#1-Cd(1)-O(1)#1	91.65(6)
Cd(1)-O(5)#1	2.330(3)	Cl(4)#1-Cd(1)-O(5)#1	90.08(8)
Cd(2)-Cl(4)	2.5320(11)	O(1)#1-Cd(1)-O(5)#1	83.57(9)
Cd(2)-O(2)	2.207(3)	Cl(4)-Cd(2)-O(2)	95.91(8)
Cd(2)-O(7)	2.300(3)	Cl(4)-Cd(2)-O(7)	88.03(6)
Cd(2)-O(8)	2.313(2)	Cl(4)-Cd(2)-O(8)	93.17(6)
Cd(2)-O(9)	2.359(3)	Cl(4)-Cd(2)-O(9)	99.61(8)
Cd(2)-O(10)	2.303(3)	Cl(4)-Cd(2)-O(10)	171.04(8)
Cl(4)-Cd(1)-O(1)	91.65(6)	O(2)-Cd(2)-O(7)	175.97(10)
Cl(4)-Cd(1)-O(5)	90.08(8)	O(2)-Cd(2)-O(8)	91.36(10)
Cl(4)-Cd(1)-Cl(4)#1	180.00	O(2)-Cd(2)-O(9)	88.62(11)
Cl(4)-Cd(1)-O(1)#1	88.35(6)	O(2)-Cd(2)-O(10)	92.43(11)
Cl(4)-Cd(1)-O(5)#1	89.92(8)	O(7)-Cd(2)-O(8)	89.25(8)
O(1)-Cd(1)-O(5)	83.57(9)	O(7)-Cd(2)-O(9)	89.90(10)
Cl(4)#1-Cd(1)-O(1)	88.35(6)	O(7)-Cd(2)-O(10)	83.68(10)
O(1)-Cd(1)-O(1)#1	180.00	O(8)-Cd(2)-O(9)	167.15(10)

Table S5. Thermal gravimetric analysis (TGA) data for compounds **1**-**3**, **6** -**8**.

Compound	% weight loss (T[^{o}C])
1	38.49 (483)
2	40.90 (507)
3	47.71 (430)
6	7.3 (160), 6.5 (290), 14.4 (420)
7	7.20 (350), 42 (420)
8	7.11 (130), 41 (600)